Defence Research and Development Canada
Recherche et développement pour la défense Canada

DRDC | RDDC

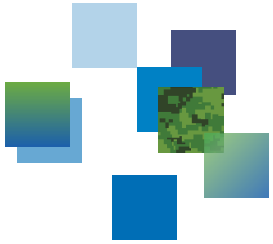

Expected challenge levels for chemical vapour standoff sensing

Eugene Yee
DRDC – Suffield Research Centre

Defence Research and Development Canada

Scientific Report
DRDC-RDDC-2016-R044
April 2016

Canada

Expected challenge levels for chemical vapour standoff sensing

Eugene Yee
DRDC – Suffield Research Centre

Defence Research and Development Canada
Scientific Report
DRDC-RDDC-2016-R044
April 2016

Abstract

In this report, challenge levels in the form of path-integrated concentrations (relevant for the assessment of standoff chemical detection performance) and in the form of partial dosages (relevant for the assessment of human exposure) have been computed and documented for three different atmospheric conditions: namely, for a moderately unstable atmospheric stratification, for a near neutral atmospheric stratification, and for a moderately stable atmospheric stratification. A model for mapping the path-integrated concentration in a toxic agent cloud into the differential spectral radiance observed by a passive Fourier-transform infrared spectrometer (applied as a standoff chemical detector) is obtained. Using the challenge levels and this model, a systematic procedure for addressing the following question is provided: can a toxic agent vapour cloud be detected by the standoff chemical detector to provide sufficient advanced warning to permit the donning of protective equipment before the exposure exceeds some critical threshold as to result in some deleterious effect on exposed personnel (co-located with the detector)? A detailed example illustrating the application of this procedure is provided.

Significance for defence and security

The expected challenge concentration data and the methodology developed to use this data provide critical information that will be needed in the definition activities associated with the specification of the required detection limits of a standoff chemical agent sensor. This information can be used to assess the mission requirements for wide-area chemical agent surveillance and to guide the development of standoff chemical sensor concepts-of-use for each mission.

Résumé

Nous avons calculé et documenté les concentrations de provocation sous la forme de concentrations intégrées sur une trajectoire (pertinentes pour l'évaluation du rendement de la détection à distance de produits chimiques) et de doses partielles (pertinentes pour l'évaluation de l'éxposition humaine) dans trois conditions atmosphériques : une stratification modérément instable, une stratification quasi neutre et une stratification modérément stable. Nous avons dérivé un modèle pour cartographier la concentration intégrée sur la trajectoire d'un nuage d'agent toxique, sous la forme d'une radiance spectrale observée par un spectromètre pour l'infrarouge à transformée de Fourier passif (utilisé comme détecteur à distance de produits chimiques). Nous proposons une procédure systématique fondée sur des concentrations de provocation et le modèle pour répondre à la question suivante : Un capteur à distance de produits chimiques peut-il détecter un nuage de vapeur d'un agent toxique et sonner l'alerte assez tôt pour que le personnel à proximité puisse enfiler son équipement de protection avant que le degré d'exposition excède un seuil critique entraînant des effets nocifs ? Nous donnons un exemple détaillé de l'application de cette procédure.

Importance pour la défense et la sécurité

Les données de concentrations de provocation attendues et la méthode élaborée d'utilisation de ces données constituent des informations cruciales qui seront nécessaires lors de la définition de la spécification des limites nécessaires de détection d'un capteur à distance d'agents chimiques. On pourra utiliser ces informations pour évaluer les exigences de mission pour la surveillance d'un agent chimique sur une zone étendue et pour guider l'élaboration de concepts d'utilisation de capteurs à distance de produits chimiques pour chaque mission.

Table of contents

List of figures

This page intentionally left blank.

1 Introduction

Following the September 11th terrorist attacks on the World Trade Center and the Pentagon, the prospect of a terrorist or state actor resorting to the use of a chemical agent that can potentially cause massive casualties and overwhelm the available emergency facilities is a problem of increasing concern. An important defensive posture against this particular threat is the development of remote detection and advanced warning of chemical warfare agent vapours following the putative release of these highly toxic agents into the atmosphere. Towards this objective, passive Fourier-transform infrared (FTIR) spectroscopy has been used for the detection and identification of gaseous contaminants released into the atmosphere that include both civil emergency (e.g., chemical accidents) and military (e.g., chemical warfare agent detection under battlefield conditions) applications.

A significant effort has been expended in development of fast and reliable methods for the remote detection of various gaseous constituents in the atmosphere based on FTIR spectroscopy related to the detection of pollutants such as sulfur oxides (SO_x), nitrogen oxides (NO_x), carbon dioxide (CO_2) and various volatile organic compounds arising from human activity (e.g., industrial releases, greenhouse gases) and natural phenomena (e.g., volcanic eruptions, wildfires). Notable advances in this respect have been made by Hilton et al. [1], Love et al. [2], Beil et al. [3], Harig and Matz [4], Lavoie et al. [5], amongst others. In comparison to point detection methods which only sense the presence of chemical vapours under local conditions, standoff detection by passive FTIR spectroscopy which can sense the presence of (toxic) chemical vapours at a distance have a number of advantages, including the potential for wide-area chemical surveillance coupled with fast scanning of the toxic agent cloud with no sample preparation or handling and no contamination of the sensor during the measurement.

The primary objective of this report is to provide path-integrated concentration data associated with the release of a toxic gas (e.g., chemical warfare agent, toxic industrial material) into the turbulent atmosphere. The path-integrated concentration data is obtained using a state-of-the-art atmospheric dispersion model. This data can be used to provide the information needed in the definition activities associated with the specification of the required detection limits of a standoff chemical sensor (and, more specifically, a passive infrared FTIR spectrometer for standoff detection which is the predominant methodology utilized for remote chemical sensing).

2 Experimental design

For passive FTIR spectrometry, the path-integrated concentration through the dispersing cloud of toxic material along the "line-of-sight" (LOS) of the sensor is the primary integrated optical property of the cloud that is required for determination (assessment) of whether the standoff chemical detector is able detect the cloud. To determine expected challenge levels of the path-integrated concentration through a toxic agent cloud dispersing in the turbulent atmosphere, we will consider the following release scenario. The release scenario involves the explosive dissemination of a toxic agent from a localized source with a mass of Q kg. The localized source is located 0.5 m above the ground surface. It is assumed that the toxic agent is instantaneously vapourized with no loss in the mass (viz., the dissemination efficiency is 100 percent). The initial cloud size at the release is assumed to be 1.0 m in all coordinate directions. In other words, the x (or alongwind), the y (or crosswind) and the z (or vertical) dimensions of the initial cloud denoted $\sigma_{x,0}$, $\sigma_{y,0}$ and $\sigma_{z,0}$, respectively, are assumed to be 1.0 m so $\sigma_{x,0} = \sigma_{y,0} = \sigma_{z,0} = 1.0$ m. The concentration distribution $\chi_0(x, y, z)$ in the initial cloud is represented as a three-dimensional Gaussian distribution with spreads $\sigma_{x,0}$, $\sigma_{y,0}$ and $\sigma_{z,0}$ in the x-, y-, and z-directions, respectively, with the functional form (Q units of matter released)

$$\chi_0(x, y, z) = \frac{Q}{(2\pi)^{3/2}\sigma_{x,0}\sigma_{y,0}\sigma_{z,0}} \exp\left[-\frac{1}{2}\left(\frac{x^2}{\sigma_{x,0}^2} + \frac{y^2}{\sigma_{y,0}^2} + \frac{z^2}{\sigma_{z,0}^2}\right)\right]. \tag{1}$$

The positive x-direction corresponds to the west-east direction, the positive y-direction corresponds to the south-north direction, and the positive z-direction to the vertical direction above the ground surface. With this Cartesian coordinate system, the release location is given by $(0, 0, 0.5)$ m.

The toxic agent cloud is released into a turbulent atmospheric boundary layer characterized by horizontally homogeneous mean wind and turbulence statistics that are considered to be fully developed over a level and unobstructed terrain. The surface roughness z_0 of the terrain was assumed to be 0.01 m which corresponds to grassland or cropland. The atmospheric dispersion model used for the determination of the cloud concentration is kinematic and requires knowledge of the wind statistics whenever dispersion is calculated. In this study, the dispersion of the initial toxic agent cloud is determined for three different atmospheric stability (or, thermal stratification) conditions: namely, (1) moderately unstable conditions (corresponding roughly to Pasquill stability category B); (2) near neutral conditions (corresponding to Pasquill stability category D); and, (3) moderately stable conditions (corresponding roughly to Pasquill stability category F).

The moderately unstable atmospheric condition corresponds to a release on a sunny afternoon with strong insolation. Under these conditions, the average wind speed U

in the surface layer adjacent to the ground is well described by Monin-Obukhov similarity theory (assumed to be directed in the x-direction corresponding to a westerly wind):

$$U(z) = \frac{u_*}{\kappa}\left[\log\left(\frac{z}{z_0}\right) + \psi_m\left(\frac{z}{L}\right)\right], \qquad L < 0, \tag{2}$$

where u_* is the friction velocity, $\kappa \approx 0.4$ is von Karman's constant, L is the Monin-Obukhov length, and $\psi_m(z/L)$ is a function that depends on height (given by z) and stratification (given by L) which for an unstable atmosphere ($L < 0$) is parameterized as follows:

$$\psi_m\left(\frac{z}{L}\right) = -2\log\left(\frac{1+\phi}{2}\right) - \log\left(\frac{1+\phi^2}{2}\right) + 2\tan^{-1}(\phi) - \frac{\pi}{2} \tag{3}$$

where $\phi \equiv (1 - 15z/L)^{1/4}$. For the simulation of dispersion in a moderately unstable atmosphere, the atmospheric boundary layer depth was specified to be $z_i = 1000$ m, the Monin-Obukhov length was specified to be $L = -12.5$ m, and the mean wind speed at 10 m above the ground surface (viz., at $z = 10$ m) was chosen to be 2.0 m s^{-1} implying a friction velocity of $u_* \approx 0.12$ m s^{-1}.

The (near) neutral atmospheric condition corresponds to either a daytime or nighttime release under strong winds and overcast conditions. The average wind speed in the surface layer under these conditions is given by Eq. (2) with $\psi_m(z/L) = 0$. For a (near) neutral atmospheric stratification, we assumed that $L = -1000$ m and that the height of the atmospheric boundary layer was $z_i = 800$ m (with no mass exchange across z_i). The average wind speed at 10 m above the ground surface was assumed to be 4.0 m s^{-1}, implying a friction velocity $u_* \approx 0.23$ m s^{-1}.

The moderately stable atmospheric condition corresponds to a nighttime release with weak surface winds under a (nearly) clear sky condition (cloud cover less than about 3/8). The average wind speed in the surface layer is given by Eq. (2) with the stability function $\psi_m(z/L)$ given by

$$\psi_m\left(\frac{z}{L}\right) = \frac{4.7z}{L}, \qquad L > 0. \tag{4}$$

For the moderately stable stratification, it is assumed that the height of the mixed layer is $z_i = 65$ m and that the Monin-Obukhov length $L = 13$ m. The mean wind speed at 10 m above the ground was chosen to be $U = 2.0$ m s^{-1}, implying that the friction velocity $u_* \approx 0.074$ m s^{-1}.

Let $\chi(x, y, z, t)$ denote the instantaneous concentration in the dispersing cloud at receptor location $\mathbf{x} \equiv (x, y, z)$ and time t after the initial release (assumed to occur at time $t = 0$). An atmospheric dispersion model predicts the ensemble-averaged concentration $\langle\chi(x, y, z, t)\rangle$ in the dispersing cloud. For standoff chemical detection, the

integrated optical property of the dispersing cloud that is relevant to the assessment of the detection limits of the sensor is the path-integrated (mean) concentration $\langle \chi_L \rangle$ through the cloud defined as follows:

$$\langle \chi_L(\mathbf{x}_s, t) \rangle = \int_0^1 \Big\langle \chi\Big(\mathbf{x}_s + \lambda\Big(\mathbf{x}_L - \mathbf{x}_s\Big), t\Big) \Big\rangle \, d\lambda, \tag{5}$$

where $\mathbf{x}_s \equiv (x_s, y_s, z_s)$ is the location of the standoff chemical detector (passive FTIR spectrometer), $\mathbf{x}_L \equiv (x_s + r\cos\alpha\sin\beta, y_s + r\cos\alpha\cos\beta, z_s + r\sin\alpha)$ is the terminal (final) location defining the path-integrated concentration. The terminal location $\mathbf{x}_L$ is determined relative to the location of the standoff chemical detector (start location) and is defined in terms of the range r and the line of sight of the sensor specified in terms of an elevation angle α (taken to be positive above the horizontal) and an azimuthal angle β (taken to be positive from the north- or y-direction). In the simulations conducted herein to determine the path-integrated concentration, the standoff chemical detector is assumed to be mounted on a tripod at a height of $h \equiv z_s = 1.5$ m above the (level) ground surface. Furthermore, it is assumed that the line of sight of the detectors is oriented so that it is "staring" horizontally at the approaching cloud. For the assumed westerly wind, the line of sight of the detector is given by $\alpha = 0$ (staring horizontally) and $\beta = 3\pi/2$ (looking west).

For a line of sight of the detector staring horizontally, the range r in the path integral of Eq. (5) is limited by the distance to the horizon (viz., the dispersing cloud cannot be 'seen' by the detector when the cloud is below the horizon along the light of sight). The distance to the horizon can be determined as follows [6]:

$$r = R_e \tan\left(\sec^{-1}\left(1 + \frac{h}{R_e}\right)\right), \tag{6}$$

where $R_e \approx 6378.137$ km is the equatorial radius of the Earth. Using $h = 1.5$ m (height of the sensor above the ground), Eq. (6) yields a range $r \approx 4.374$ km. The path-integrated concentration $\langle \chi_L \rangle$ was determined as a function of time t (measured from when the instantaneous release occurred) at four downwind distances from the source along the cloud centerline. More specifically, the path-integrated concentration was determined (for each of the three atmospheric conditions summarized above) at the following locations: $\mathbf{x}_s \equiv (x_s, y_s, z_s) = (2000, 0, 1.5)$, $(3000, 0, 1.5)$, $(4000, 0, 1.5)$ and $(5000, 0, 1.5)$ m.

To assess the toxic effects for the released agent, the mean partial dosage $\langle \chi_D \rangle$ was also calculated from the mean cloud concentration. The partial dosage is defined as follows:

$$\langle \chi_D(\mathbf{x}, t) \rangle = \int_0^t \Big\langle \chi(\mathbf{x}, t') \Big\rangle \, dt', \qquad t > 0. \tag{7}$$

In addition to the path-integrated concentration, the partial dosage at the locations of the standoff chemical detector were computed also. More specifically, $\langle \chi_D \rangle$ was

computed at $\mathbf{x} = \mathbf{x}_s$ for $\mathbf{x}_s$ corresponding to the four receptor locations enumerated above.

The atmospheric transport and diffusion of the chemical agent vapour for the release scenario (described previously) is modeled using the Hazard Prediction and Assessment Capability (HPAC) Modeling System [7]. HPAC is an integrated package of software modules that consists of: (1) source term models for estimating the amount, rate, form and physical state of hazardous material releases from weapons or facilities; (2) modules that permit the use of high-resolution weather (meteorological), terrain, and land use (cover) data; (3) an advanced puff diffusion model used for the prediction of the atmospheric transport and diffusion of released materials; and, (4) modules for the determination of collateral effects of the downwind transport and distribution of hazardous materials on the exposed population. The output from HPAC represents a "best estimate" (or, prediction) of the hazard resulting from the released material in terms of location and coverage, evolution of the hazard with time, and collateral human effects with respect to the assumptions used in the modeling (e.g., terrain, atmospheric conditions, source characteristics, etc.).

The atmospheric dispersion model used in HPAC is the Second-order Closure Integrated Puff (SCIPUFF) model [8], which is a puff diffusion model that relates dispersion rate to velocity fluctuation statistics in the atmosphere, the latter of which uses a turbulence diffusion parameterization based on second-order turbulence closure theory. The model releases a number of individual Gaussian puffs of pollutant to represent an arbitrary three-dimensional, time-dependent (ensemble-averaged) concentration field. The puffs are subsequently advected (moved) by the mean wind field over a three-dimensional grid representing a discretization of the computational domain. The wind input may be derived from several types of meteorological input, including surface and upper air observations or three-dimensional gridded wind data obtained from a weather forecasting or mesoscale model. Atmospheric boundary-layer turbulence is determined explicitly in terms of surface heat flux and shear stress using parameterized profile shapes.

SCIPUFF simulates the instantaneous cloud or plume characteristics by adding the concentration contributed by the individual Gaussian puffs, growing in size as they are advected (or, transported) by the mean wind field. The model utilizes an efficient scheme for splitting puffs (when they grow too large for single point meteorology to be representative) and merging puffs (when there is an excessive number of puffs in the computational domain). In consequence, the puff model is able to predict complex time- and space-varying concentration distributions in actual wind conditions.

The Analytical Incident tool in HPAC was used to design (build) the release described earlier at the beginning of this section. Owing to the fact that the release was instantaneous and the measurement of the path-integrated concentration by the

standoff chemical detector is near instantaneous (viz., the duration of the sampling time associated with any given measurement is very short), the dispersion of the cloud was calculated using a conditional averaging time of zero. This implies that we calculate the concentration distribution in an instantaneous snapshot of the dispersing cloud whereby the effects of the large-scale eddies associated with the meandering component of the turbulence is neglected, with the result that the cloud dispersion is due only to the small-scale diffusion effects of the turbulence. In other words, the model results obtained herein represent the relative cloud dispersion in the limit of short time averages of the path-integrated concentration acquired by the standoff chemical detector. HPAC was applied with a conditional averaging time of zero to determine the ensemble-mean concentration $\langle \chi(\mathbf{x}, t) \rangle$ in the dispersing cloud, and this averaged concentration was used subsequently in conjunction with Eqs (5) and (7) to determine the ensemble-averaged path-integrated concentration and partial dosage, respectively.

3 Results

The normalized ensemble-averaged path-integrated concentration $\langle \chi_L(\mathbf{x}_s, t) \rangle \Big/ Q$ and the normalized ensemble-averaged partial dosage $\langle \chi_D(\mathbf{x}, t) \rangle \Big/ Q$ are displayed in Figs 1, 2 and 3, as a function of the time t since the initial release (at $t = 0$ s) for a cloud dispersing, respectively, under moderately unstable atmospheric conditions (Pasquill stability category B), under nearly neutral atmospheric conditions (Pasquill stability category D) and under moderately stable atmospheric conditions (Pasquill stability category F). The results for the path-integrated concentration are obtained for a standoff chemical detector located along the mean cloud centerline ($y_s = 0$) at a height of $z_s = 1.5$ m above ground level and at four different downwind distances from the release location; namely, at $x_s = 2000$, 3000, 4000, and 5000 m. The partial dosages were computed at four receptor locations corresponding to the locations of the standoff chemical detector (viz., at $\mathbf{x} = \mathbf{x}_s$). The path-integrated concentration was obtained for a sensor that is "looking" horizontally and directly upwind through the central core of the approaching cloud providing, as such, the expected maximum values for $\langle \chi_L \rangle$ at any time t after the release.

The dispersing cloud lies within the event horizon (recall that the distance to the horizon was determined in Section 2 to be $r = 4374$ m) of the standoff chemical detectors at $x_s = 2000$, 3000 and 4000 m downwind of the instantaneous release. For these three standoff chemical detectors, the entire cloud can be "seen" by the detectors and, generally speaking, the path-integrated concentration $\langle \chi_L \rangle$ is a monotonically decreasing function of the time t since the initial release event. It is noted that there are two rates of decrease in $\langle \chi_L \rangle$, one rate associated with the early phase of dispersion and another rate associated with the late phase of dispersion. The rate of decrease in

$\langle \chi_L \rangle$ in the early phase of dispersion corresponds to the situation where the leading (front) edge of the dispersing cloud is upwind of the location of the standoff chemical detector. It is seen that this rate of decrease is slower than the rate of decrease in $\langle \chi_L \rangle$ associated with the late phase of dispersion corresponding to the situation where the front edge of the cloud has already advected past the location of the standoff chemical detector.

The dispersing cloud initially lies beyond the event horizon of the standoff chemical detector located at $x_s = 5000$ m downwind of the instantaneous release (recall the distance to the horizon is $r = 4374$ m). For an initial portion of the early phase of dispersion, the cloud is located outside the event horizon of this detector, with the result that $\langle \chi_L \rangle = 0$. Once the front edge of the cloud appears within the event horizon, the path-integrated concentration increases rapidly to a maximum value corresponding to the time $t = t_*$ when the entire cloud is inside the event horizon of the sensor. After this time ($t > t_*$), the temporal evolution of $\langle \chi_L \rangle$ resembles that observed by the detectors at $x_s = 2000$, 3000 and 4000 m (in which the cloud always lies within the event horizon). Again, note that for the detector at $x_s = 5000$ m, $\langle \chi_L \rangle$ is a monotonically decreasing function of t for $t > t_*$. Furthermore, this function exhibits two distinct rates of decrease corresponding to the early phase of dispersion when the leading edge of the cloud is upwind of the detector at $x_s = 5000$ m and to the late phase of dispersion when the leading edge of the cloud is downwind of the location of the detector.

All other conditions being the same, it is noted that $\langle \chi_L \rangle$ and $\langle \chi_D \rangle$ are smaller at a given time t the more unstable the stratification in the atmosphere (viz., these two quantities are smaller for dispersion in a moderately unstable atmosphere than for that in a moderately stable atmosphere). Furthermore, the rates of decrease in the early and late phases of dispersion in $\langle \chi_L \rangle$ are smaller for dispersion in a more stably stratified atmosphere.

4 Applications

The results of Section 3 document the temporal evolution of the path-integrated concentration $\langle \chi_L \rangle$ and the partial dosage $\langle \chi_D \rangle$ at a number of fixed locations downwind of the instantaneous release. The path-integrated concentration can be used to assess the detectability of the cloud at a given time after the initial release, whereas the partial dosage can be used to assess the potential exposure to the toxic material of the cloud at a given time after the initial release. The information embodied in $\langle \chi_L \rangle$ and $\langle \chi_D \rangle$ can be jointly utilized to address the following critical question: can the approaching cloud be detected by the standoff chemical detector to provide sufficient advanced warning to permit donning of protective equipment before the exposure exceeds some critical threshold as to result in some deleterious effect on exposed

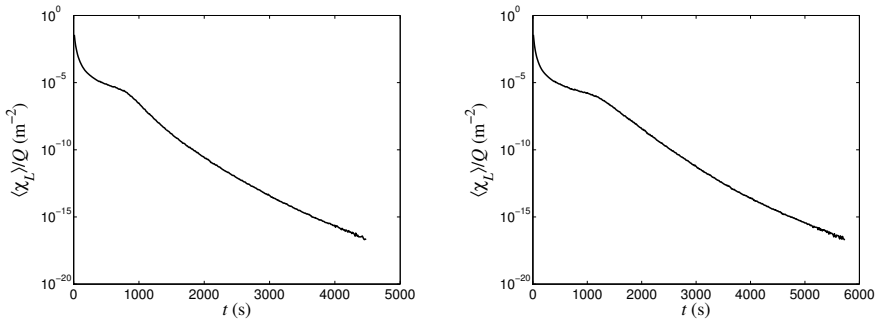

(a) $(x_s, y_s, z_s) = (2000, 0, 1.5)$ m

(b) $(x_s, y_s, z_s) = (3000, 0, 1.5)$ m

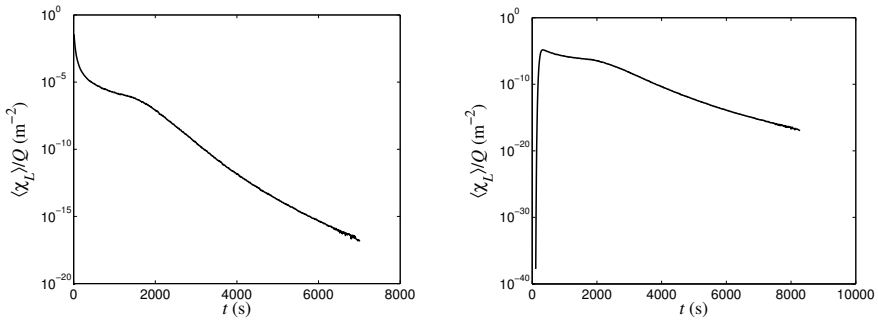

(c) $(x_s, y_s, z_s) = (4000, 0, 1.5)$ m

(d) $(x_s, y_s, z_s) = (5000, 0, 1.5)$ m

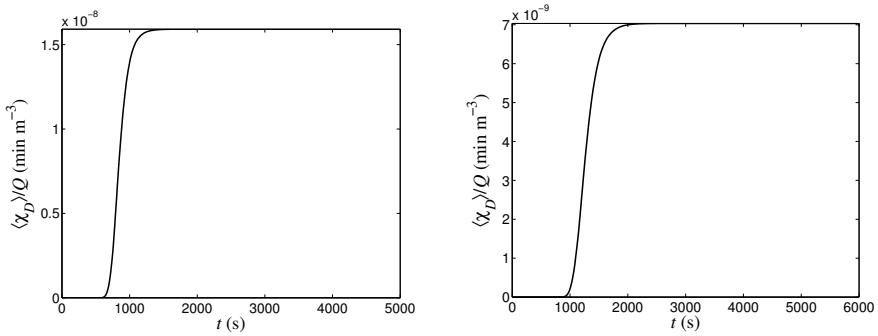

(e) $(x_s, y_s, z_s) = (2000, 0, 1.5)$ m

(f) $(x_s, y_s, z_s) = (3000, 0, 1.5)$ m

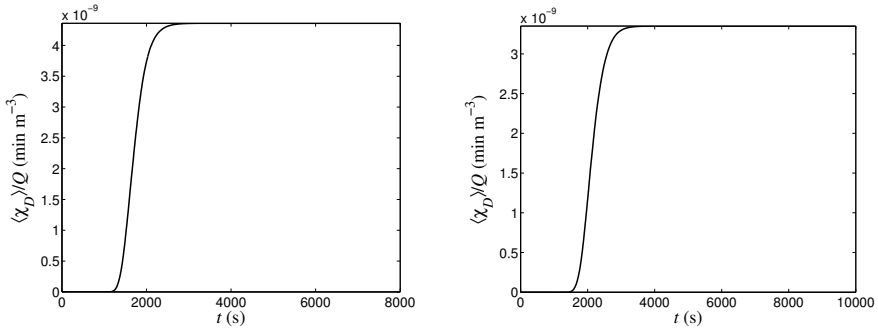

(g) $(x_s, y_s, z_s) = (4000, 0, 1.5)$ m

(h) $(x_s, y_s, z_s) = (5000, 0, 1.5)$ m

Figure 1: (a)–(d) Normalized ensemble-averaged path-integrated concentration $\langle \chi_L \rangle / Q$ (Q is the mass of toxic gas released) as a function of time t after the initial release ($t = 0$ s) for a standoff chemical detector located at (x_s, y_s, z_s); (e)–(h) normalized ensemble-averaged partial dosage $\langle \chi_D \rangle / Q$ as a function of time t after the initial release at a receptor location given by (x_s, y_s, z_s). The results are for the dispersion of the cloud under moderately unstable atmospheric conditions.

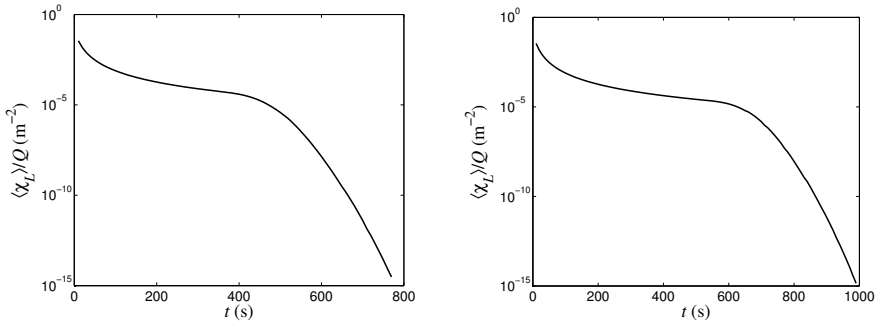

(a) $(x_s, y_s, z_s) = (2000, 0, 1.5)$ m

(b) $(x_s, y_s, z_s) = (3000, 0, 1.5)$ m

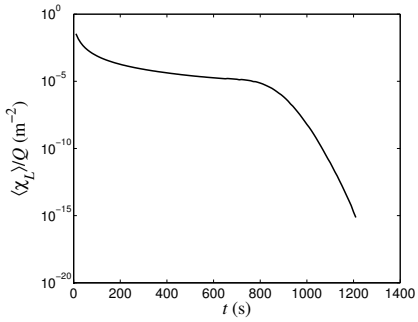

(c) $(x_s, y_s, z_s) = (4000, 0, 1.5)$ m

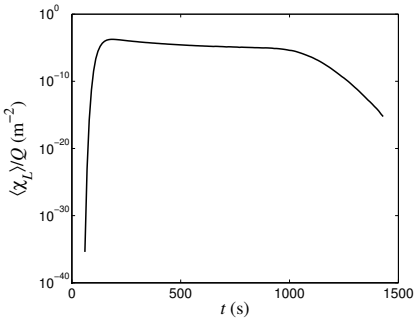

(d) $(x_s, y_s, z_s) = (5000, 0, 1.5)$ m

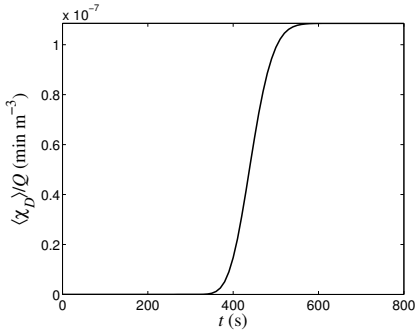

(e) $(x_s, y_s, z_s) = (2000, 0, 1.5)$ m

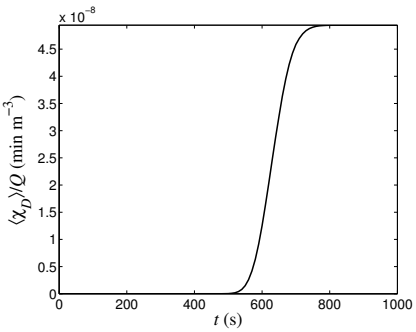

(f) $(x_s, y_s, z_s) = (3000, 0, 1.5)$ m

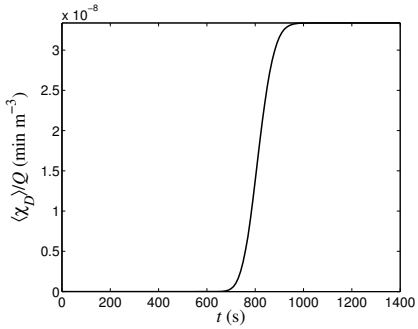

(g) $(x_s, y_s, z_s) = (4000, 0, 1.5)$ m

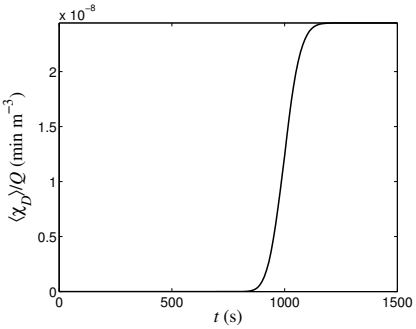

(h) $(x_s, y_s, z_s) = (5000, 0, 1.5)$ m

Figure 2: (a)–(d) Normalized ensemble-averaged path-integrated concentration $\langle \chi_L \rangle / Q$ (Q is the mass of toxic gas released) as a function of time t after the initial release ($t = 0$ s) for a standoff chemical detector located at (x_s, y_s, z_s); (e)–(h) normalized ensemble-averaged partial dosage $\langle \chi_D \rangle / Q$ as a function of time t after the initial release at a receptor location given by (x_s, y_s, z_s). The results are for the dispersion of the cloud under (nearly) neutral atmospheric conditions.

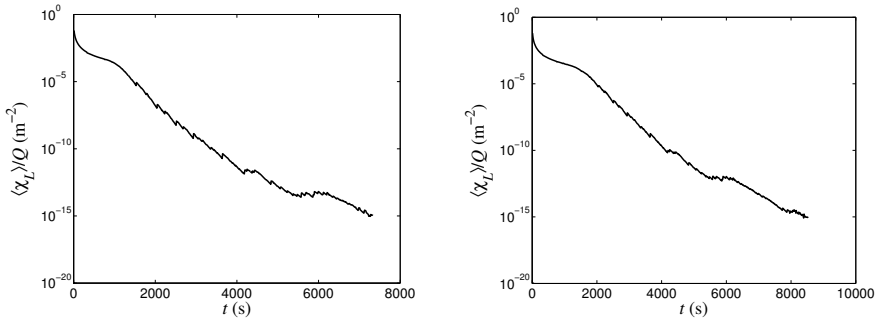

(a) $(x_s, y_s, z_s) = (2000, 0, 1.5)$ m (b) $(x_s, y_s, z_s) = (3000, 0, 1.5)$ m

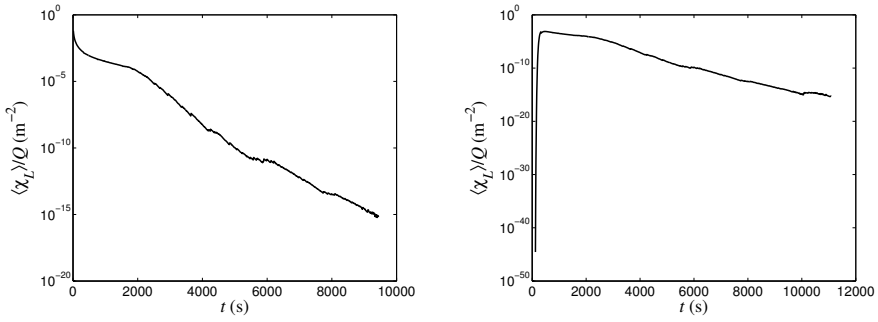

(c) $(x_s, y_s, z_s) = (4000, 0, 1.5)$ m (d) $(x_s, y_s, z_s) = (5000, 0, 1.5)$ m

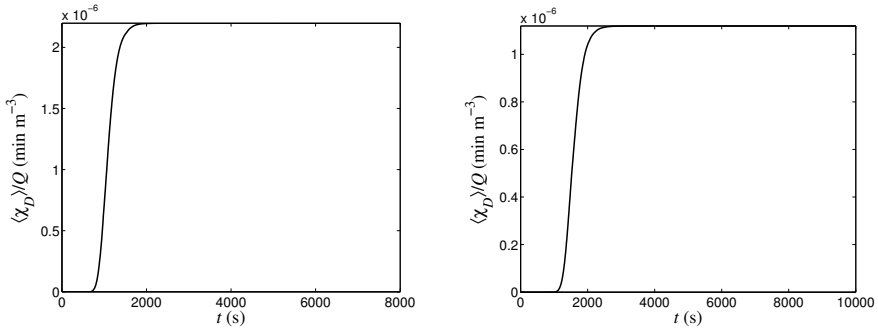

(e) $(x_s, y_s, z_s) = (2000, 0, 1.5)$ m (f) $(x_s, y_s, z_s) = (3000, 0, 1.5)$ m

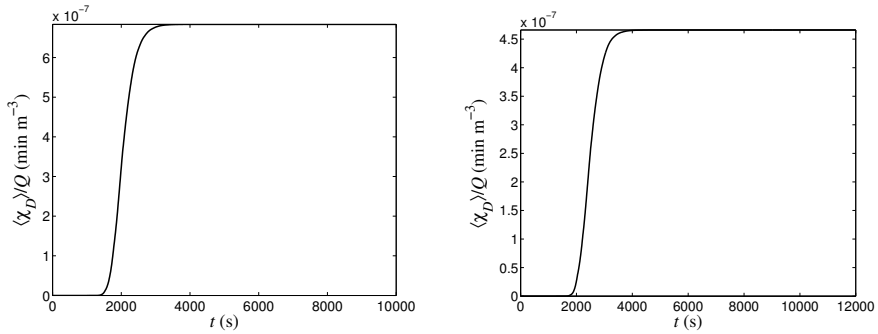

(g) $(x_s, y_s, z_s) = (4000, 0, 1.5)$ m (h) $(x_s, y_s, z_s) = (5000, 0, 1.5)$ m

Figure 3: (a)–(d) Normalized ensemble-averaged path-integrated concentration $\langle \chi_L \rangle / Q$ (Q is the mass of toxic gas released) as a function of time t after the initial release ($t = 0$ s) for a standoff chemical detector located at (x_s, y_s, z_s); (e)–(h) normalized ensemble-averaged partial dosage $\langle \chi_D \rangle / Q$ as a function of time t after the initial release at a receptor location given by (x_s, y_s, z_s). The results are for the dispersion of the cloud under moderately stable atmospheric conditions.

personnel (co-located with the detector)? The purpose of this section is to provide an example of how the results documented in Section 3 can be used to address this question.

Firstly, we focus on the detectability of the cloud and this will require a mapping of the path-integrated concentration into the spectral radiance that is measured by the standoff chemical detector (assumed to be a passive FTIR spectrometer for the purposes of this analysis). To this purpose, we require a radiative transfer model for the dispersing cloud in the atmosphere. Following the lead of Beer [9], we consider a model of the dispersing cloud in the atmosphere which is partitioned into three plane-parallel homogeneous layers along the optical path. The first layer is the background layer, the second layer is the toxic cloud layer (consisting of a mixture of the toxic vapor molecules and air), and the third layer is the atmospheric layer consisting of the atmosphere lying between the leading (front) edge of the toxic cloud and the spectrometer.

The background spectral radiance L_1 from the sky in the first (background) layer enters the second layer at the trailing (back) edge of the toxic cloud. The spectral radiance L_2 exiting from the second (cloud) layer is given by

$$L_2 = \tau_C L_1 + (1 - \tau_C) L_2^{bb}, \tag{8}$$

where τ_C is the transmittance and L_2^{bb} is the spectral radiance of the toxic agent cloud. The first term in Eq. (8) corresponds to the transmittance through the second layer and the second term in Eq. (8) represents the emittance from the second layer. The reflectance (due to scattering) from a toxic vapour cloud in the infrared spectral range is negligible, so that the emittance ϵ_C of the cloud is related to the transmittance as $\epsilon_C = (1 - \tau_C)$. All quantities in Eq. (8) are assumed implicitly to depend on the wavenumber k of the radiation.

The spectral radiance L_3 exiting the third (atmospheric) layer and entering the spectrometer is given by

$$L_3 = \tau_A L_2 + (1 - \tau_A) L_3^{bb}, \tag{9}$$

where τ_A is the transmittance through the atmospheric layer and L_3^{bb} is the spectral radiance of the atmospheric layer. Inserting Eq. (8) into Eq. (9) leads to

$$L_3 = \tau_A \Big(\tau_C L_1 + (1 - \tau_C) L_2^{bb} \Big) + (1 - \tau_A) L_3^{bb}. \tag{10}$$

It is assumed that the spectral radiance from the background (sky) L_1 can be approximated as a blackbody at temperature T_{sky} (which can be determined using the standard Planck's function). Furthermore, it is assumed that the spectral radiance from the toxic agent cloud L_2^{bb} and from the atmosphere L_3^{bb} are blackbodies at the temperature of the cloud T_C and at the temperature of the atmosphere T_A, respectively. Finally, it is expected that there will be rapid entrainment of air into the

dispersing toxic agent cloud, so $T_C = T_A$ to a very good approximation implying that $L_2^{bb} = L_3^{bb} \equiv B_C$. Furthermore, it is assumed that transmittance through the atmospheric layer lying between the leading edge of the cloud and the spectrometer is unity (viz., $\tau_A = 1$). Inserting these assumptions into Eq. (10) yields finally

$$L_3 = B_C + \tau_C(L_1 - B_C). \tag{11}$$

The key quantity that determines whether the toxic agent cloud can be detected by the FTIR spectrometer is the contrast between spectral radiance L_3 measured at the entrance of the detector and the spectral radiance L_1 of the background. From Eq. (11), the differential spectral radiance $\Delta L \equiv L_3 - L_1$ is given by

$$\Delta L \equiv L_3 - L_1 = (1 - \tau_C)(B_C - L_1) \equiv (1 - \tau_C)\Delta L_{Cb}. \tag{12}$$

The transmittance through the toxic agent cloud is given by the Lambert-Beer law [9]:

$$\tau_C(k) = \exp\Big(-\xi(k)\langle\chi_L\rangle\Big), \tag{13}$$

where the explicit dependence of τ_C on the wavenumber k of the radiation is indicated and $\xi(k)$ is the absorptivity (mass absorption cross section) of the toxic agent vapour. Eqs (12) and (13) show that the detection of the presence of the toxic agent cloud depends on two primary factors: namely, (1) on the path-integrated concentration $\langle\chi_L\rangle$ as manifested through the cloud transmittance τ_C; and, (2) on the difference between the cloud temperature T_C and the background (sky) temperature $T_{\rm sky}$ as manifested through $\Delta L_{Cb} \equiv (B_C - L_1)$ (essentially a thermal contrast between the cloud and the background owing to the fact that the spectral radiances B_C and L_1 are considered to be blackbody emitters).

A FTIR spectrometer has a finite resolution owing to the finite movement of the mirror in the interferometer, which imposes an upper bound on the maximum optical path difference in the interferometer. As a result, the actual measured differential spectral radiance ΔL_M is the convolution of the ideal differential spectral radiance ΔL [cf. Eq. (12)] with the instrument line shape of the spectrometer [10]:

$$\Delta L_M(k) = \Delta L(k) \star A(k), \tag{14}$$

where $\star$ denotes the convolution operation and the apparatus function A is given by

$$A(k) = 2D\mathrm{sinc}(2\pi Dk). \tag{15}$$

Here, D is the maximum optical path difference in the interferometer and $\mathrm{sinc}(x) \equiv \sin(x)/x$.

For the assessment of the detection limits of the FTIR spectrometer, we select the peak value k_0 in the absorptivity spectrum for the toxic agent. This corresponds to the

wavenumber of the radiation associated with the minimum value of the transmittance through the cloud. Inserting Eqs (12), (13) and (15) into Eq. (14) and assuming that the shape of the spectral line at k_0 can be approximated by a Lorentzian profile, the measured differential spectral radiance $\Delta L_M(k_0)$ evaluated at $k = k_0$ can be shown (after some straightforward manipulations) to be given by

$$\Delta L_M(k_0) = \Delta L_{Cb}(k_0) \int_{-\infty}^{\infty} \left(1 - \exp\left(-\frac{\xi(k_0)\langle\chi_L\rangle\tilde{\gamma}^2}{\tilde{\gamma}^2 + \phi^2}\right)\right) \frac{\sin\pi\phi}{\pi\phi}\, d\phi. \tag{16}$$

In Eq. (16), $\tilde{\gamma} \equiv \Gamma\big/\Delta\sigma$ is the ratio of the full-width at half maximum Γ of the Lorentzian spectral line at $k = k_0$ to the spectral resolution $\Delta\sigma \equiv 1/D$ of the spectrometer. It is noted that Eq. (16) is the required mapping from the ensemble-averaged path-integrated concentration $\langle\chi_L\rangle$ [cf. Eq. (5)] to the expected differential spectral radiance observed by the spectrometer (at the wavenumber corresponding to the dominant peak in the absorptivity spectrum of the toxic agent cloud).

Whether the toxic agent cloud can be detected or not depends on whether $|\Delta L_M(k_0)|$ significantly exceeds the instrument noise level. To this purpose, it is useful to consider the noise equivalent spectral radiance of the instrument. The noise equivalent spectral radiance (NESR) of a spectrometer is given by [10], [11]:

$$\text{NESR} = \frac{2A_D^{1/2}}{\Theta\eta\Delta\sigma D^*(\delta t)^{1/2}}, \tag{17}$$

where A_D is the detector area, Θ is the étendue, η is the optical system efficiency, $\Delta\sigma$ is the nominal spectral resolution of the instrument (which is proportional to the equivalent width of the instrument line shape), D^* is the specific detectivity of the instrument, and δt is the measurement time (viz., the sampling time over which spectra acquired by the instrument are averaged).

One can declare that the toxic agent cloud is detected if $|\Delta L_M(k_0)| > \zeta \cdot \text{NESR}$, where ζ is a pre-selected factor by which $|\Delta L_M(k_0)|$ must exceed the NESR before the toxic agent is declared to be present in the measurement. The selection of the noise threshold ζ will determine the false-alarm rate for the detector. Of course, setting the threshold ζ to a smaller value will increase the probability that the threat agent cloud is detected, but will also result in a higher false-alarm rate. As with any detection system, there will always be a tradeoff between the probability that the toxic agent cloud will be detected and the probability of false alarm. For example, if it is assumed that the instrument noise is Gaussian with a mean of zero and a standard deviation equal to the NESR, then the choice $\zeta = 5$ will imply that the probability of false alarm is 5.73×10^{-7} (or, equivalently, assuming that spectra are acquired by the detector every $\delta t = 1$ s, we expect one false alarm to be issued after every 20.2 d of continuous operation).

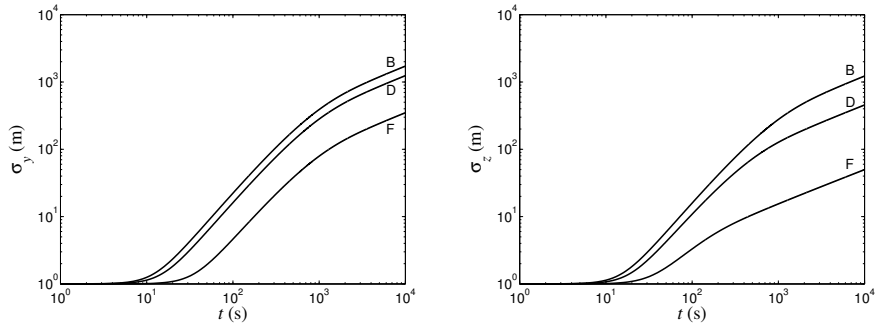

(a) (b)

Figure 4: Temporal evolution of the (a) cloud diffusion width $\sigma_y(t)$ in the lateral or y-direction and (b) cloud diffusion width $\sigma_z(t)$ in the vertical or z-direction for moderately unstable (Pasquill category B), near neutral (Pasquill category D), and moderately stable (Pasquill category F) atmospheric conditions.

With respect to the detection of the toxic agent cloud, there is one further factor that needs to be taken into account. Even though $|\Delta L_M(k_0)| > \zeta \cdot \text{NESR}$, the cloud may not be detected owing to the fact that the "size" of the cloud may be so small that it "fills" only a very small (insignificant) fraction of the entire field of view (FOV) of the detector. To this purpose, we consider the fill fraction (or, fill factor) f which is simply a measure of the fraction of the field of view of the detector that is "filled" by the threat agent cloud when a measurement is made (at time t). This fill fraction f is defined as follows:

$$f(t) = \min\left\{1, \frac{4\sigma_y(t)\sigma_z(t)}{\Big(\|\mathbf{x}_s - \mathbf{x}_c(t)\| \cdot \theta\Big)^2}\right\}, \tag{18}$$

where $\sigma_y(t)$ and $\sigma_z(t)$ are the cloud diffusion widths in the y- and z-directions, respectively, at time t; $\mathbf{x}_s$ is the location of the standoff chemical detector; $\mathbf{x}_c(t)$ is the location of the cloud centroid at time t; θ is the angular measure of the field of view of the detector; and, $\|\cdot\|$ denotes the Euclidean distance. In Eq. (18), it is assumed implicitly that the threat agent cloud is advected along the positive x-direction and that the line of sight of the standoff chemical detector is along the negative x-direction ("staring" directly at the approaching cloud), with the result that the size of the cloud normal to the line of sight of the detector is determined by the lateral cloud width σ_y and the vertical cloud width σ_z.

Figure 4 exhibits the cloud diffusion widths σ_y and σ_z as a function of time t for a toxic agent cloud dispersing in a moderately unstable (Pasquill stability category B), near neutral (Pasquill stability category D), and moderately stable (Pasquill stability category F) atmospheric boundary layer. The cloud diffusion widths were derived from the ensemble-averaged concentration $\langle\chi(x, y, z, t)\rangle$ determined earlier in

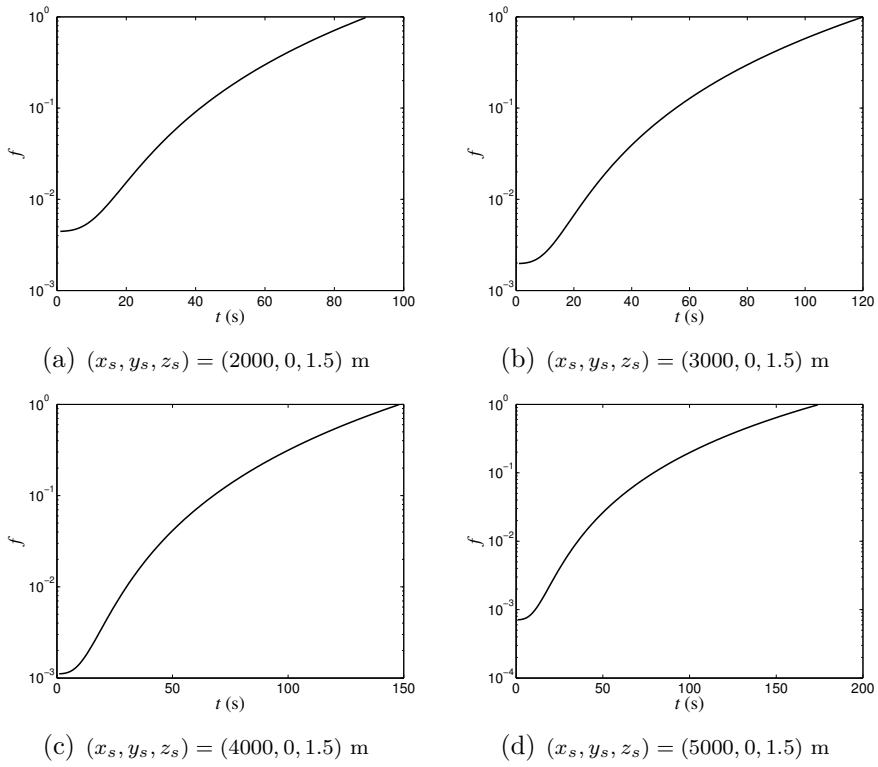

(a) $(x_s, y_s, z_s) = (2000, 0, 1.5)$ m

(b) $(x_s, y_s, z_s) = (3000, 0, 1.5)$ m

(c) $(x_s, y_s, z_s) = (4000, 0, 1.5)$ m

(d) $(x_s, y_s, z_s) = (5000, 0, 1.5)$ m

Figure 5: Fill fraction f associated with cloud diffusion in a moderately unstable atmosphere for a standoff chemical detector located at (x_s, y_s, z_s).

Section 3. The cloud diffusion widths can be used in conjunction with Eq. (18) to determine the fill fraction f (again with the cloud centroid location $\mathbf{x}_c(t)$ derived from $\langle \chi(x, y, z, t) \rangle$ computed earlier). Figures 5, 6 and 7 display the temporal evolution of f for standoff chemical detectors positioned at four locations directly downwind of the initial release (x_s = 2000, 3000, 4000 and 5000 m) and for a toxic agent cloud dispersing in a moderately unstable, near neutral and moderately stable atmospheric boundary layer, respectively. These results have been computed for a detector with an angular measure of the field of view of $\theta = 15$ mrad.

Up to this point, the focus has been on the determination of whether the toxic agent cloud can be detected by the standoff chemical detector and this aspect has utilized the information embodied in the path-integrated concentration $\langle \chi_L \rangle$. Going on with this procedure, we need to determine whether a person co-located with the standoff chemical detector will experience some deleterious effect before the threat cloud can be detected and an early warning provided. Towards this objective, the information embodied in the partial dosage $\langle \chi_D \rangle$ will be utilized.

A number of toxicity/health exposure guidelines have been specifically established to support emergency planning and response decision to protect the public. One set

of general guidelines for toxic materials is the Protective Action Criteria (PAC) [12] which describes the dangers to humans resulting from short-term exposure to airborne chemicals. The PAC values have been compiled by the United States Department of Energy and are based on chemical exposure limit values provided in the Acute Exposure Guideline Levels (AEGLs, final and interim), the Emergency Response Planning Guidelines (ERPGs), and the Temporary Emergency Exposure Limits (TEELs) data sets. The PAC values include three concentration levels representing different effect severity levels. The three PAC values which are appropriate for an exposure duration t_e of one hour have been defined as follows:

• **PAC-1** is the airborne concentration (expressed as parts per million or milligrams per cubic meter (ppm or mg m^{-3})) of a substance above which it is predicted that the general population, including susceptible individuals, could experience notable discomfort, irritation, or certain asymptomatic non-sensory effects. However, the effects are not disabling and are transient and reversible upon cessation of exposure.

• **PAC-2** is the airborne concentration (expressed as ppm or mg m^{-3}) of a substance above which it is predicted that the general population, including susceptible individuals, could experience irreversible or other serious, long-lasting adverse health effects or an impaired ability to escape.

• **PAC-3** is the airborne concentration (expressed as ppm or mg m^{-3}) of a substance above which it is predicted that the general population, including susceptible individuals, could experience life-threatening health effects or death.

Given a specific level of effect, say PAC-x, the information embodied in the normalized partial dosage $\langle\chi_D\rangle\big/Q$ (see Figs 1–3) can be used to determine the mass of toxic material Q that needs to be released in the explosive dissemination in order that a receptor at a given (fixed) location downwind of the release experiences that effect. For the assessment considered herein, we will use the total dosage $\langle\chi_D\rangle_T$ to determine Q. The total dosage is defined to be the value of the partial dosage taken at a time t sufficiently large that the toxic agent cloud has completely passed over the given receptor location [viz., $\langle\chi_D\rangle_T = \lim_{t\to\infty}\langle\chi_D(t)\rangle$]. For a given level of effect, the amount of matter Q needed to produce that effect at a particular (fixed) receptor location $\mathbf{x}$ is given by

$$Q = \frac{(\text{PAC-}x)t_e}{\langle\chi_D(\mathbf{x})\rangle_T\big/Q} \equiv \frac{(\text{PAC-}x)t_e}{\lim_{t\to\infty}\langle\chi_D(\mathbf{x},t)\rangle\big/Q}. \tag{19}$$

Once Q has been determined, it can be used to un-normalize $\langle\chi_L\rangle\big/Q$ in Figs 1 to 3 to give $\langle\chi_L\rangle$ which can be subsequently used in Eq. (16) to determine the differential spectral radiance observed by the standoff chemical detector. This information, used

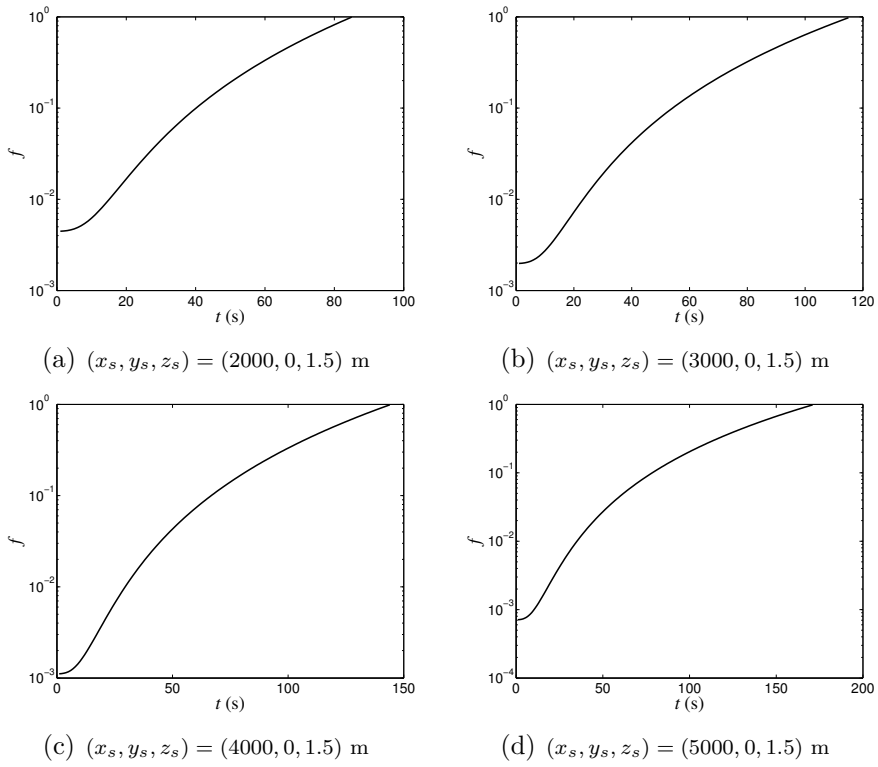

(a) $(x_s, y_s, z_s) = (2000, 0, 1.5)$ m

(b) $(x_s, y_s, z_s) = (3000, 0, 1.5)$ m

(c) $(x_s, y_s, z_s) = (4000, 0, 1.5)$ m

(d) $(x_s, y_s, z_s) = (5000, 0, 1.5)$ m

Figure 6: Fill fraction f associated with cloud diffusion in a near neutral atmosphere for a standoff chemical detector located at (x_s, y_s, z_s).

in conjunction with the NESR and the fill fraction f, can be used to assess whether the detector can detect the toxic agent cloud and issue an advanced warning before an exposed person co-located with the detector will have experienced a specified level of effect.

We are, at last, ready to put all the pieces together and formally state the procedure:

1. For the toxic agent of concern, determine the specific level of effect PAC-x for this agent [12]. For a given receptor location, determine the total dosage $\langle \chi_D \rangle_T$ at this location (cf. Figs 1–3) for the particular state of the atmosphere (unstable, neutral, stable) and use Eq. (19) to determine the amount of matter Q that needs to be released to produce the specific level of effect at the receptor location.

2. For the toxic agent of concern, extract the wavenumber k_0 associated with the dominant (largest) peak in the absorptivity spectrum for the agent and the value of the absorptivity $\xi(k_0)$ at this wavenumber. Extract the full width at half maximum Γ for this spectral peak.

3. Using the value of Q determined in Step 1, un-normalize $\langle \chi_L \rangle \big/ Q$ (cf. Figs 1–3)

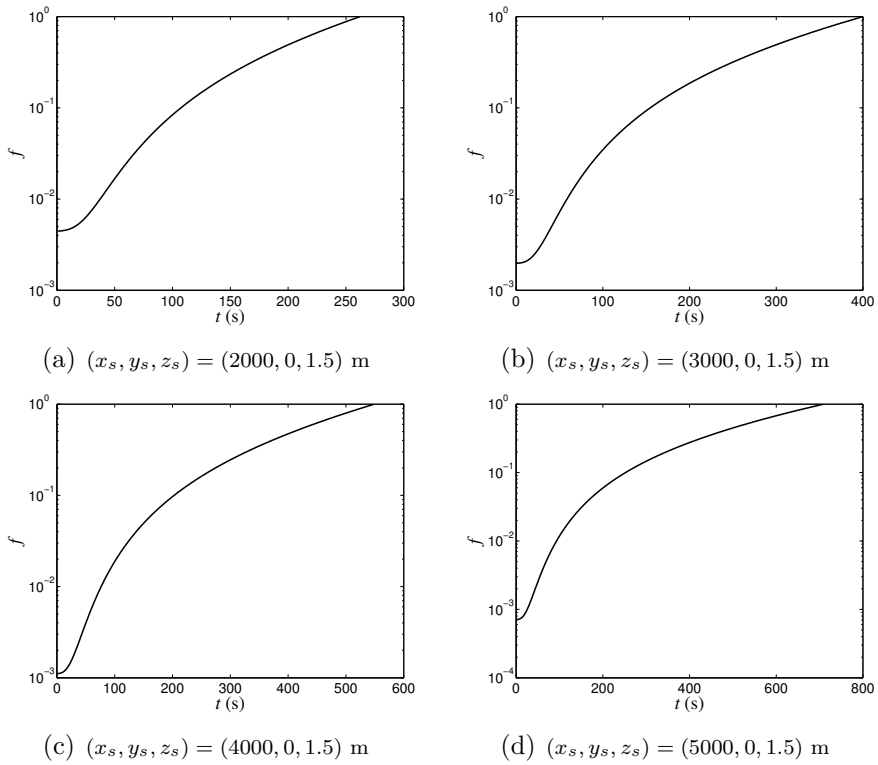

(a) $(x_s, y_s, z_s) = (2000, 0, 1.5)$ m

(b) $(x_s, y_s, z_s) = (3000, 0, 1.5)$ m

(c) $(x_s, y_s, z_s) = (4000, 0, 1.5)$ m

(d) $(x_s, y_s, z_s) = (5000, 0, 1.5)$ m

Figure 7: Fill fraction f associated with cloud diffusion in a moderately stable atmosphere for a standoff chemical detector located at (x_s, y_s, z_s).

at the given receptor location and for the particular state of the atmosphere.

4. Specify the temperature of the background (sky) T_{sky} and the temperature of the cloud T_C (the latter of which is assumed to be equal to the temperature of the atmosphere given the rapid entrainment of air into the dispersing cloud). Using these temperatures, compute the blackbody[1] spectral radiances for the background (sky) L_1 and for the toxic agent cloud B_C at the wavenumber k_0. Use this information to compute $\Delta L_{Cb}(k_0) \equiv (B_C(k_0) - L_1(k_0))$ [cf. Eq. (12)].

5. Specify the characteristics of the FTIR spectrometer: (a) spectral resolution

[1]Recall that the spectral radiance L from a blackbody at wavenumber k and (absolute) temperature T can be computed from Planck's function which is given by

$$L(k,T) = \frac{C_1 k^3}{\exp\big(C_2 k/T\big) - 1} \ ,$$

where $C_1 \equiv 2hc^2 = 1.191 \times 10^{-12}$ W cm^{-2} sr^{-1} (cm^{-1})$^{-4}$ and $C_2 \equiv hc/k_B = 1.439$ K cm are the first and second radiation constants. Here, h is Planck's constant, c is the speed of light, and k_B is Boltzmann's constant.

$\Delta\sigma$ of the instrument; (b) the NESR for the instrument or, equivalently, the instrument parameters A_D, Θ, η, D^* and δt which can be used in conjunction with Eq. (17) to compute the NESR.

6. Use the information in Steps 2, 3, 4, and 5(a) to compute $\Delta L_M(k_0)$ in accordance to Eq. (16).

7. Specify the noise threshold level factor ζ. Find the interval of time $(t_{1<}, t_{1>})$ for which the constraint $|\Delta L_M(k_0)| > \zeta \cdot \text{NESR}$ is satisfied, where the NESR is determined from Step 5(b) and $\Delta L_M(k_0)$ is determined from Step 6.

8. Specify a minimum value $f_{\min}$ for the fill fraction which must be exceeded before a toxic agent cloud is deemed to be detected. Using the information in Figs 5 to 7 for the given state of the atmosphere, determine the smallest time $t_{2,*}$ for which $f(t) > f_{\min}$. Compute the interval $I \equiv (t_{1<}, t_{1>}) \bigcap (t_{2,*}, \infty) \equiv (t_<, t_>)$. For the given receptor location and state of the atmosphere, find the time t_f at which the partial dosage $\langle \chi_D(t) \rangle$ first attains its maximum value (this value being the total dosage $\langle \chi_D \rangle_T$). This information is embodied in Figs 1 to 3. If $I \neq \emptyset$ (where $\emptyset$ denotes the empty set) and $t_< < t_f$, then the toxic agent cloud can be detected before the specific level of effect has been reached at the receptor location; otherwise, the toxic agent cloud can not be detected for the given conditions.

4.1 Example

To illustrate the application of the procedure, let us apply it to the standoff detection of a toxic cloud consisting of the nerve agent isopropyl methylphosphonofluoridate (sarin or GB). In accordance with Step 1 of the procedure, we consider a receptor (detector) location $(x_s, y_s, z_s) = (5000, 0, 1.5)$ for a moderately unstable and a moderately stable stratification in the atmosphere. The specific level of effect will be chosen to be the PAC-2 level for sarin which according to Table 2 (Protective Action Criteria, Rev. 27 dated February 2012) [12] is found to be 2.04 mg min m^{-3} ($\equiv$ PAC-2 $\cdot\, t_e$, with an exposure duration $t_e = 60$ min). Using the information embodied in Figs 1(h) and 3(h) in conjunction with Eq. (19), the values of Q required to produce a PAC-2 level of effect at the given receptor for a moderately unstable and a moderately stable atmospheric stratification are, respectively, 608.8 kg and 1.8226 kg.

With reference to Step 2 of the procedure, the absorptivity spectrum for sarin has been measured by Williams et al. [13]. From the measured absorptivity spectrum for sarin with a wavenumber range from 500 cm^{-1} to 4000 cm^{-1}, the largest peak in the spectrum was found to occur at $k_0 = 1020.9$ cm^{-1} and the value of the absorptivity coefficient at this wavenumber was found to be $\xi(k_0) = (5.96 \pm 0.04) \times 10^{-4}$ m^2 mg^{-1}.

For this spectral line, the full width at half maximum was found to be $\Gamma = 30$ cm^{-1} ($\pm 10\%$).

The values of Q determined in Step 1 were used in conjunction with the information embodied in Figs 1(d) and 3(d) to obtain the path-integrated concentration $\langle \chi_L \rangle$ (Step 3 of the procedure). With reference to Step 4 of the procedure, we specify a temperature for background (sky) of $T_{\text{sky}} = 293$ K. Two different temperatures for the toxic agent cloud (or, equivalently, temperatures of the atmosphere) are considered; namely, $T_C = 295$ K and $T_C = 293.5$ K providing a thermal contrast between the background (sky) and the cloud of 2 K and 0.5 K, respectively. With this specification for the temperatures of the background and cloud, the blackbody spectral radiances for the background L_1 and the cloud B_C were computed at the wavenumber k_0 (determined in Step 2), and used to determine $\Delta L_{Cb}(k_0)$.

For Step 5 of the procedure, we need to specify instrument parameters for the standoff chemical detector. To this purpose, the detector is assumed to have a spectral resolution of $\Delta\sigma = 10$ cm^{-1} (implying a maximum optical path difference in the interferometer of $D = 0.1$ cm). The other relevant instrument parameters are as follows: $A_D = 0.01$ cm^2, $\Theta = 0.0082$ cm^2 sr, $\eta = 0.1$, $D^* = 4 \times 10^{10}$ cm Hz$^{1/2}$ W^{-1}, and $\delta t = 1$ s.[2] Using these values of the instrument parameters, the NESR for the instrument is determined using Eq. (17) to be NESR $= 6.0976 \times 10^{-10}$ W cm^{-2} sr^{-1} (cm^{-1})$^{-1}$.

Using the information determined in Steps 2 to 5 above, the observed differential spectral radiance $\Delta L_M(k_0)$ was computed using Eq. (16) (Step 6 of the procedure). The results of this calculation are summarized in Fig. 8 for moderately unstable and stable atmospheric stratifications and for two different thermal contrasts between the temperature of the background (sky) and temperatures of the cloud (or, atmosphere); namely, for thermal contrasts of 2 K and 0.5 K. The time corresponding to the first "kink" in the $\Delta L_M(k_0)$ curves shown in Fig. 8 is associated with the time when the entire toxic sarin cloud is contained within the event horizon of the standoff chemical detector (viz., the cloud is entirely above the horizon and within the line of sight of the detector). The time t corresponding to the second "kink" in the $\Delta L_M(k_0)$ curves is associated with the time (approximately or better) when the leading (front) edge of the toxic sarin cloud has advected past the detector location.

Moving on to Step 7 of the procedure, we will choose $\zeta = 5$ implying that the relevant noise threshold for detection of the cloud is $\zeta \cdot \text{NESR} = 30.488 \times 10^{-10}$ W cm^{-2} sr^{-1} (cm^{-1})$^{-1}$. Using the information embodied in Fig. 8 (determined in Step 6 of the procedure), we can now determine the interval $(t_{1<}, t_{1>})$ where the constraint $|\Delta L_M(k_0)| > \zeta \cdot \text{NESR}$ is verified. The intervals $(t_{1<}, t_{1>})$ are determined for the

[2]These are generic but representative parameters for a hypothetical spectrometer, and do not necessarily correspond to any real commercially-available spectrometer.

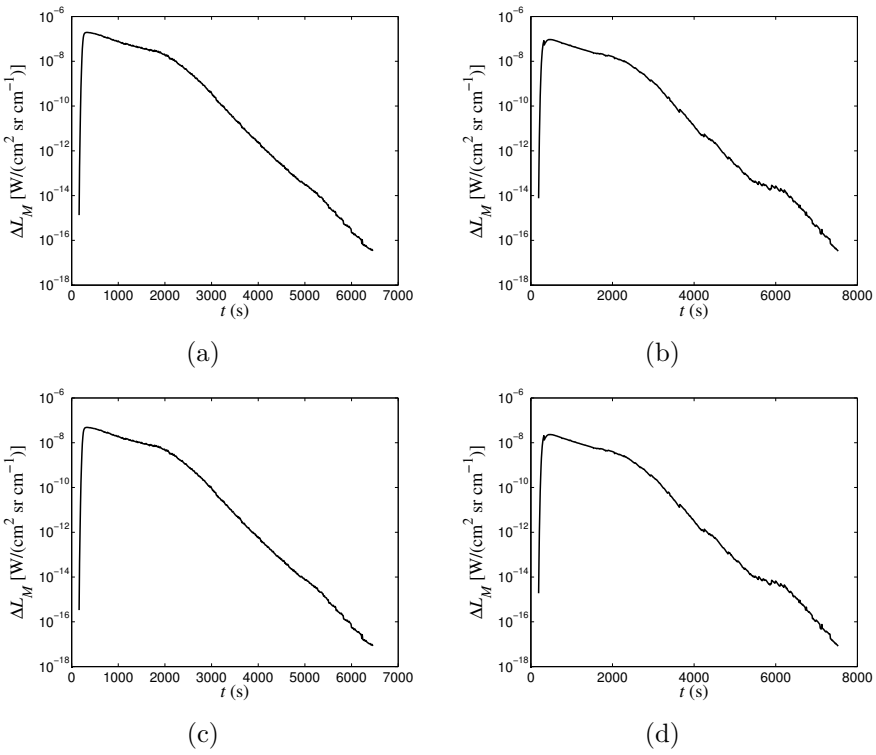

Figure 8: Observed differential spectral radiance $\Delta L_M(k_0)$ for standoff chemical detector at $(x_s, y_s, z_s) = (5000, 0, 1.5)$ m corresponding to a toxic sarin cloud ($k_0 = 1020.9$ cm^{-1}) dispersing in the atmosphere: (a) moderately unstable atmosphere with a thermal contrast of 2 K; (b) moderately stable atmosphere with a thermal contrast of 2 K; (c) moderately unstable atmosphere with a thermal contrast of 0.5 K; and, (d) moderately stable atmosphere with a thermal contrast of 0.5 K.

four cases shown in Fig. 8 and are found to be given by: (a) $(210, 2550)$ s for the moderately unstable atmosphere with a thermal contrast of 2 K; (b) $(250, 2720)$ s for the moderately stable atmosphere with a thermal contrast of 2 K; (c) $(220, 2160)$ s for the moderately unstable atmosphere with a thermal contrast of 0.5 K; and, (d) $(270, 2140)$ s for the moderately stable atmosphere with a thermal contrast of 0.5 K.

Finally, for Step 8 of the procedure, we select $f_{\min} = 0.2$ implying that the toxic sarin cloud needs to be large enough that it will fill 20% of the entire field of view of the spectrometer before a detection will be declared. Now, using Figs 5(d) and 7(d), it can be determined that at the receptor location $(x_s, y_s, z_s) = (5000, 0, 1.5)$ m, the smallest time $t_{2,*}$ for which $f > f_{\min}$ is $t_{2,*} \approx 100$ s and 340 s, respectively, for the moderately unstable and stable atmosphere. Given $t_{2,*}$ and the information determined in Step 7, the interval $I = (t_{1<}, t_{1>}) \bigcap (t_{2,*}, \infty)$ can be determined.

The intervals I for the four cases shown in Fig. 8 are given by: (a) $(210, 2550)$ s for

the moderately unstable atmosphere with a thermal contrast of 2 K; (b) $(340, 2720)$ s for the moderately stable atmosphere with a thermal contrast of 2 K; (c) $(220, 2160)$ s for the moderately unstable atmosphere with a thermal contrast of 0.5 K; and, (d) $(340, 2140)$ s for the moderately stable atmosphere with a thermal contrast of 0.5 K. The interval I corresponds to the interval of time for which the differential spectral radiance from the toxic sarin cloud exceeds the noise threshold and for which the cloud is large enough to fill at least 20% of the entire field of view for the detector.

From Figs 1(h) and 3(h), the time t_f when the total dosage is "received" at the receptor location $(x_s, y_s, z_s) = (5000, 0, 1.5)$ m is seen to be about 3810 s and 3880 s for the moderately unstable and moderately stable atmosphere, respectively. For the example considered here, this total dosage corresponds to the PAC-2 level for sarin. It should be realized that for each of the four cases documented in Fig. 8, t_f exceeds the times associated with the interval I implying that the toxic sarin cloud for these four cases can be detected and an advanced warning issued to take protective action before the dosage reaches the PAC-2 level for sarin at the receptor location.

5 Conclusions

In this report, a methodology has been developed to address the following question: can a toxic gas cloud dispersing in the atmosphere be detected by a standoff chemical detector and an early warning issued to take appropriate protective action before the exposure of personnel co-located with the detector exceeds some critical threshold as to result in some deleterious effect? To address this question rigorously, expected challenge levels in the form of the path-integrated concentration and the partial dosage were computed using a state-of-the-art atmospheric dispersion model for three different atmospheric conditions: namely, a moderately unstable atmosphere, a near neutral atmosphere, and a moderately stable atmosphere. The path-integrated concentration provides the critical information required to assess the detection performance of a standoff chemical detector and the partial dosage provides the critical information required to assess the toxic effects on exposed personnel.

A model for the mapping of the path-integrated concentration into the differential spectral radiance measured (observed) by a standoff chemical detector (more, specifically, a passive FTIR spectrometer) has been developed. Using the challenge levels and this model, a systematic procedure for addressing the question posed above has been developed. A detailed example illustrating the application of this procedure is provided. The example (case) considered here uses sarin as the toxic material, and describes in detail how to apply all the steps of the procedure for this case. It would be useful to extend the methodology to investigate the standoff detection of toxic liquid chemical agents (having negligible vapour pressure) and of toxic solid chemical agents released as a liquid or solid aerosol, respectively.

References

[1] Hilton, M., Lettington, A. H., and Mills, I. M. (1993), Passive remote detection of atmospheric pollutants using Fourier Transform Infrared (FTIR) spectroscopy, *Proceedings of the SPIE*, 2089, 314–315.

[2] Love, S. P., Goff, F., Counce, D., Siebe, C., and Delgado, H. (1998), Passive infrared spectroscopy of the eruption plume at Popocatépetl volcano, Mexico, *Nature*, 396, 563–567.

[3] Beil, A., Daum, R., Harig, R., and Matz, G. (1998), Remote sensing of atmospheric pollution by passive FTIR spectroscopy, *Proceedings of the SPIE*, 3493, 32–43.

[4] Harig, R. and Matz, G. (2001), Toxic cloud imaging by infrared spectroscopy: a scanning FTIR system for identification and visualization, *Field Analytical Chemistry and Technology*, 5, 75–90.

[5] Lavoie, H., Puckrin, E., Theriault, J. M., and Bouffard, F. (2005), Passive standoff detection of SF_6 at a distance of 5.7 km by differential Fourier transform infrared radiometry, *Applied Optics*, 59, 1189–1193.

[6] Wolfram Alpha: Computational Knowledge Engine (online), `http://www.wolframalpha.com` (Access Date: May 2013).

[7] Science Applications International Corporation (1999), Hazard Prediction and Assessment Capability (HPAC), HPAC-UGUIDE-01-U-RAC0, Defense Threat Reduction Agency (DTRA).

[8] Sykes, R. I., Parker, S. F., Henn, D. S., and Chowdhury, B. (2006), SCIPUFF Version 2.2: Technical Documentation, (Technical Report A.R.A.P Report No. 729) L-3 Titan Corporation.

[9] Beer, R. (1992), *Remote Sensing by Fourier Transform Spectroscopy*, Wiley, New York.

[10] Harig, R. (2004), Passive remote sensing of pollutant clouds by FTIR spectrometry: Signal-to-noise ratio as a function of spectral resolution, *Applied Optics*, 43, 4603–4610.

[11] Flanigan, D. F. (1995), Vapor-detection sensitivity as a function of spectral resolution for a single Lorentzian band, *Applied Optics*, 34, 2636–2639.

[12] Protection Action Criteria (PAC): Chemicals with AEGLs, ERPGs, and TEELs (online), `http://www.atlintl.com/doe/teels/teel_archives.html` (Access Date: March 2016).

[13] Williams, B. R., Hulet, M. S., Samuels, A. C., and Miles, J. A. (2009), Vapor-phase infrared absorptivity coefficient of isopropyl methylphosphonfluoridate, (Technical Report ECBC TR 696) Edgewood Chemical Biological Center.

DOCUMENT CONTROL DATA

(Security markings for the title, abstract and indexing annotation must be entered when the document is Classified or Designated.)

1. ORIGINATOR (The name and address of the organization preparing the document. Organizations for whom the document was prepared, e.g., Centre sponsoring a contractor's report, or tasking agency, are entered in section 8.)

DRDC – Suffield Research Centre
Box 4000, Station Main, Medicine Hat AB T1A 8K6, Canada

2a. SECURITY MARKING (Overall security marking of the document, including supplemental markings if applicable.)

UNCLASSIFIED

2b. CONTROLLED GOODS

(NON-CONTROLLED GOODS)
DMC A
REVIEW: GCEC APRIL 2011

3. TITLE (The complete document title as indicated on the title page. Its classification should be indicated by the appropriate abbreviation (S, C or U) in parentheses after the title.)

Expected challenge levels for chemical vapour standoff sensing

4. AUTHORS (Last name, followed by initials – ranks, titles, etc. not to be used.)

Yee, E.

5. DATE OF PUBLICATION (Month and year of publication of document.)	6a. NO. OF PAGES (Total containing information. Include Annexes, Appendices, etc.)	6b. NO. OF REFS (Total cited in document.)
April 2016	34	13

7. DESCRIPTIVE NOTES (The category of the document, e.g., technical report, technical note or memorandum. If appropriate, enter the type of report, e.g., interim, progress, summary, annual or final. Give the inclusive dates when a specific reporting period is covered.)

Scientific Report

8. SPONSORING ACTIVITY (The name of the department project office or laboratory sponsoring the research and development – include address.)

DRDC – Suffield Research Centre
Box 4000, Station Main, Medicine Hat AB T1A 8K6, Canada

9a. PROJECT OR GRANT NO. (If appropriate, the applicable research and development project or grant number under which the document was written. Please specify whether project or grant.)	9b. CONTRACT NO. (If appropriate, the applicable number under which the document was written.)
FE 03 Inform Project (2.3.1, 2.3.2, 2.3.3)	

10a. ORIGINATOR'S DOCUMENT NUMBER (The official document number by which the document is identified by the originating activity. This number must be unique to this document.)	10b. OTHER DOCUMENT NO(s). (Any other numbers which may be assigned this document either by the originator or by the sponsor.)
DRDC-RDDC-2016-R044	

11. DOCUMENT AVAILABILITY (Any limitations on further dissemination of the document, other than those imposed by security classification.)

(X) Unlimited distribution
( ) Defence departments and defence contractors; further distribution only as approved
( ) Defence departments and Canadian defence contractors; further distribution only as approved
( ) Government departments and agencies; further distribution only as approved
( ) Defence departments; further distribution only as approved
( ) Other (please specify):

12. DOCUMENT ANNOUNCEMENT (Any limitation to the bibliographic announcement of this document. This will normally correspond to the Document Availability (11). However, where further distribution (beyond the audience specified in (11)) is possible, a wider announcement audience may be selected.)

13. ABSTRACT (A brief and factual summary of the document. It may also appear elsewhere in the body of the document itself. It is highly desirable that the abstract of classified documents be unclassified. Each paragraph of the abstract shall begin with an indication of the security classification of the information in the paragraph (unless the document itself is unclassified) represented as (S), (C), or (U). It is not necessary to include here abstracts in both official languages unless the text is bilingual.)

In this report, challenge levels in the form of path-integrated concentrations (relevant for the assessment of standoff chemical detection performance) and in the form of partial dosages (relevant for the assessment of human exposure) have been computed and documented for three different atmospheric conditions: namely, for a moderately unstable atmospheric stratification, for a near neutral atmospheric stratification, and for a moderately stable atmospheric stratification. A model for mapping the path-integrated concentration in a toxic agent cloud into the differential spectral radiance observed by a passive Fourier-transform infrared spectrometer (applied as a standoff chemical detector) is obtained. Using the challenge levels and this model, a systematic procedure for addressing the following question is provided: can a toxic agent vapour cloud be detected by the standoff chemical detector to provide sufficient advanced warning to permit the donning of protective equipment before the exposure exceeds some critical threshold as to result in some deleterious effect on exposed personnel (co-located with the detector)? A detailed example illustrating the application of this procedure is provided.

14. KEYWORDS, DESCRIPTORS or IDENTIFIERS (Technically meaningful terms or short phrases that characterize a document and could be helpful in cataloguing the document. They should be selected so that no security classification is required. Identifiers, such as equipment model designation, trade name, military project code name, geographic location may also be included. If possible keywords should be selected from a published thesaurus. e.g. Thesaurus of Engineering and Scientific Terms (TEST) and that thesaurus identified. If it is not possible to select indexing terms which are Unclassified, the classification of each should be indicated as with the title.)

atmospheric dispersion; chemical sensing; standoff remote sensing; passive infrared

DRDC | RDDC

SCIENCE, TECHNOLOGY AND KNOWLEDGE FOR CANADA'S DEFENCE AND SECURITY | SCIENCE, TECHNOLOGIE ET SAVOIR POUR LA DÉFENSE ET LA SÉCURITÉ DU CANADA

www.drdc-rddc.gc.ca